Yersinia Entry into Host Cells Requires Rab5-Dependent Dephosphorylation of PI(4,5)P$_2$ and Membrane Scission

Helen Sarantis[1], **Daniel M. Balkin**[5], **Pietro De Camilli**[5], **Ralph R. Isberg**[6], **John H. Brumell**[1,2,3], and **Sergio Grinstein**[1,2,4,*]

[1]Cell Biology Program, Hospital for Sick Children, Toronto, Ontario M5G 1X8, Canada

[2]Institute of Medical Science

[3]Department of Molecular Genetics

[4]Department of Biochemistry, University of Toronto, Toronto, ON M5S 1A8, Canada

[5]Department of Cell Biology, Howard Hughes Medical Institute, Program In Cellular Neuroscience Neurodegeneration and Repair, Yale University School of Medicine, New Haven, CT 06510, USA

[6]Department of Molecular Biology and Microbiology, Howard Hughes Medical Institute, Tufts University School of Medicine, Boston, MA 02111, USA

Summary

Some bacteria invade host cells by triggering a process akin to phagocytosis. We analyzed the mechanisms underlying invasion vacuole formation by the bacterium *Yersinia pseudotuberculosis*. After engaging integrins on host cells, *Yersinia* resided in PI(4,5)P$_2$-rich, membrane-bound compartments called "prevacuoles" that were inaccessible to extracellular antibodies but remained connected to the plasma membrane. The scission of prevacuoles to form separate, sealed compartments coincided with and required PI(4,5)P$_2$ hydrolysis. At the time of scission, the inositol 5-phosphatases OCRL and Inpp5b were recruited to prevacuoles. This recruitment and subsequent PI(4,5)P$_2$ hydrolysis required the association of the GTPase Rab5 with prevacuoles. Phosphatidylinositol 3-kinase activity was required for fusion of Rab5-positive vesicles with prevacuoles and scission of nascent vacuoles from the plasma membrane. Thus, *Yersinia* invasion involves a multistep process in which the bacteria form a protective prevacuole and then recruit host factors to induce membrane fission, allowing the bacteria to invade the cell.

Introduction

Phagocytosis is critical for multiple aspects of development and immunity, including clearance of apoptotic cells, host defense against pathogens, and antigen presentation. Typically, phagocytosis is a receptor-driven process that involves recognition of a particulate target by the host cell, followed by actin-dependent extension of pseudopods, and culminating in particle engulfment and scission of the nascent phagosome from the plasma

membrane. Subsequently, the phagosome fuses with intracellular compartments, gradually acquiring markers of early and late endosomes, and, finally, lysosomes, in a process termed maturation (Huynh et al., 2007). Rab family GTPases direct membrane targeting during phagocytosis: Rab5 enables recruitment of early endosomes by nascent phagosomes and is also required for the recruitment of Rab7, which in turn promotes the formation of phagolysosomes (Vieira et al., 2003).

Phosphoinositides appear to play a key role in phagocytosis (Yeung and Grinstein, 2007). Activation of class I phosphatidylinositol 3-kinase (PI3K) is essential for optimal Fcγ receptor, Dectin-1, and complement receptor-mediated phagocytosis by professional phagocytes (Araki et al., 1996; Cox et al., 1999; Herre et al., 2004). Internalization of *Yersinia* by epithelial cells is similarly dependent on PI3K (Schulte et al., 1998). Class I PI3K isoforms catalyze the generation of phosphatidylinositol 3,4,5-*tris*phosphate (PI[3,4,5]P$_3$) from phosphatidylinositol 4,5-bisphydate (PI(4,5)P$_2$), accounting in part for the depletion of PI(4,5)P$_2$ that is reported to occur prior to phagosome scission (Botelho et al., 2000). In addition, hydrolysis by phospholipase C (PLC) contributes to the disappearance of PI(4,5)P$_2$ from nascent phagosomes, as indicated by the concomitant accumulation of diacylglycerol (Botelho et al., 2000). The disappearance of PI(4,5)P$_2$ coincides with actin clearance from the base of the phagocytic cup and with phagosomal sealing. Remarkably, other membrane internalization processes, such as clathrin-mediated endocytosis and macropinocytosis, are also accompanied by the disappearance of PI(4,5)P$_2$, which occurs as the vesicles or vacuoles undergo scission from the surface membrane (Di Paolo and De Camilli, 2006; Porat-Shliom et al., 2008).

Some microbial pathogens gain entry into host cells and establish a niche for intracellular survival. *Yersinia pseudotuberculosis* and *Yersinia enterocolitica* utilize their outer membrane proteins, Invasin and YadA, to engage β1 integrins and enter host cells (Isberg and Leong, 1990; Young et al., 1992). The underlying process is remarkably similar to receptor-mediated engulfment of bacteria by professional phagocytes, involving tyrosine phosphorylation (Rosenshine et al., 1992) and F-actin remodeling via activation of Rho family GTPases (Alrutz et al., 2001).

In contrast to what has been reported for other endocytic events, entry of *Yersinia* into host cells proceeds without the disappearance of PI(4,5)P$_2$, which seemingly persists on vacuoles containing internalized, antibody-inaccessible bacteria (Wong and Isberg, 2003). In this study, we examined more closely the dynamics of PI(4,5)P$_2$ during *Yersinia* entry. We show herein that *Yersinia* enters epithelial cells in a multistep manner. Following binding, the bacteria are encircled by the cell into PI(4,5)P$_2$-positive structures that remain continuous with the plasma membrane. These prevacuoles represent an intermediate step in the internalization process, at which scission from the plasma membrane has not been completed although the entrapped bacteria are segregated and protected from the extracellular milieu. The subsequent scission requires the loss of PI(4,5)P$_2$, which is brought about by the recruitment of PI(4,5)P$_2$ phosphatases that are delivered to the prevacuoles by a Rab5-dependent process.

Results

Identification of an Intermediate Stage of *Yersinia* Entry into Host Cells

To determine the fate of PI(4,5)P$_2$ during internalization of *Yersinia*, we infected COS cells expressing the pleckstrin homology (PH) domain of PLCδ fused to GFP (PH-PLCδ, a PI(4,5)P$_2$ biosensor) with Alexa 647-labeled *Y. pseudotuberculosis*. As shown in Figure S1F available online, expression of the PH probe did not affect the kinetics of *Yersinia* entry. Following termination of infection at the indicated times by fixation, extracellular adherent and/or partially internalized bacteria were identified by addition of *Yersinia*-specific antibodies followed by fluorophore-conjugated secondary antibodies. As reported by Wong and Isberg (2003), we could readily detect PI(4,5)P$_2$-positive vacuoles containing bacteria that were inaccessible to extracellular antibodies, implying that they had been internalized (Figure 1A). After 10 min, ≈70% of the vacuoles appeared to be sealed by this criterion (Figure 1D).

To confirm by independent means that bacteria were fully internalized within PI(4,5)P$_2$-positive vacuoles, we treated infected live cells with the membrane-impermeant dye FM4-64. Following infection at 37°C, staining with FM4-64 was performed rapidly (within 5 min) in the cold to prevent uptake of the dye via pinocytosis. Strikingly, when sealing was assessed in this manner, virtually every PI(4,5)P$_2$-positive structure appeared to be continuous with the plasma membrane, as suggested by colabeling with FM4-64 (Figures 1B and 1C). This observation suggests that only unsealed vacuoles contain PI(4,5)P$_2$, a conclusion that conflicts with the data obtained using antibodies. The kinetics of PI(4,5)P$_2$ disappearance from the vacuoles was similar whether sealing was assessed using FM4-64 or antibodies (Figure S1D), ruling out methodological differences, such as the inclusion/omission of a fixation step, as the source of the differences between assays. Moreover, the fraction of FM4-64-negative vacuoles was ≈5% after 5 min of infection but increased gradually as the time allowed for infection was prolonged (Figure 1D), implying that the dye is in fact impermeant but also that completion of sealing is comparatively slow. Thus, when using FM4-64 to assess scission, only those vacuoles that were still continuous with the surface membrane were found to contain PI(4,5)P$_2$.

The divergent conclusions reached by using FM4-64 and antibodies to determine sealing can be reconciled by assuming that, prior to undergoing scission, the nascent vacuoles attain an intermediate configuration with a narrow constriction that precludes free diffusion of large molecules like IgG. As a result, the existing membrane continuity would allow diffusion of FM4-64 (MW: 600 Da), whereas the constricted passage would minimize the amount of antibodies (MW: 150,000 Da) that reach bacterial epitopes. This hypothesis was tested by direct visualization of early stages of infection by transmission electron microscopy (TEM) and also using smaller molecules to assess the size of the putative constriction. As shown in Figures 1E and 1F′, incompletely sealed vacuoles could readily be found in micrographs of COS cells infected with *Yersinia* for 5 min, and many of these displayed tight apposition of the membranes that encircled the bacteria. Analysis of serial sections separated by ∼80 nm allowed us to envisage a stage in which a bacterium had been engulfed by the cells (Figure S1G, panels 5–9), although the membrane had not fully sealed (panels 1–4; see arrow).

We sought an alternative strategy that would permit fixation. Therefore, we used biotinylated bacteria and probed exposure to the extracellular medium using fluorescent streptavidin conjugates (MW: 60,000 Da). Using this method, the majority of the $PI(4,5)P_2$-positive vacuoles were accessible to the extracellular marker (Figures S1A and S1B). Quantification of invasion using streptavidin was not significantly different from that assessed by FM4-64 (Figure S1C) and, in both cases, sealing correlated with disappearance of $PI(4,5)P_2$ from the vacuoles (compare Figures S1C and S1E). These observations imply that streptavidin, which is considerably smaller than IgG, can diffuse through the narrow passage generated by the apposed membranes. We conclude that, prior to sealing, *Yersinia*-containing vacuoles acquire a transient intermediate state where their membrane remains continuous with the plasmalemma and therefore contains $PI(4,5)P_2$, although the contents are isolated from the extracellular space by a constriction with selective permeability that excludes large molecules. We refer to this intermediate structure, which temporarily segregates the pathogen from the extracellular milieu, as the "prevacuole" (Figure 1G). Scission of prevacuoles from the surface membrane is best defined as inaccessibility to FM4-64 or streptavidin, and not by staining with antibodies.

$PI(4,5)P_2$ Depletion Is Required for Scission of the Prevacuole

Our data suggest that $PI(4,5)P_2$ disappearance and scission of the prevacuole from the plasma membrane occur concomitantly. To determine whether $PI(4,5)P_2$ removal is in fact required for scission, we overexpressed phosphatidylinositol 4-phosphate 5 kinases (PIP5Ks), the enzymes responsible for $PI(4,5)P_2$ production at the plasma membrane, in an attempt to prevent depletion of the phosphoinositide during infection. Using fluorescent streptavidin, invasion was quantified in fixed cells to more accurately define the time of infection while enabling quantitation of large numbers of cells. As illustrated in Figures 2A, 2B, and S2C, overexpression of two separate PIP5K isoforms inhibited bacterial entry into cells. Phosphorylation of $PI(4)P$ to $PI(4,5)P_2$ was required for this inhibition because transfection of a kinase-dead (KD) version of PIP5Kβ had little effect on invasion (Figures 2B and S2C). Therefore, overproduction of $PI(4,5)P_2$ at the plasma membrane antagonizes vacuole formation, consistent with the notion that $PI(4,5)P_2$ hydrolysis is required for scission of the prevacuole.

PI3Ks Are Involved in Scission of *Yersinia* Prevacuoles from the Plasma Membrane

We proceeded to analyze the mechanism underlying $PI(4,5)P_2$ depletion from the sealing vacuole. $PI(4,5)P_2$ is metabolized by three main pathways in mammalian cells: 1) conversion to $PI(3,4,5)P_3$ via class I PI3Ks; 2) cleavage into inositol 3,4,5-tri-sphosphate and diacylglycerol (DAG) by PLC; and 3) dephosphorylation by inositol phosphatases. The role of PI3Ks was tested first. We performed invasion assays in the presence of the PI3K inhibitors LY294002 and wortmannin and monitored the disappearance of $PI(4,5)P_2$, the efficiency of invasion, and the morphology of the cells by TEM. The PI3K antagonists produced a marked inhibition of invasion, which was assessed using streptavidin (Figures 2D, 2E, S2B, and S2E). Remarkably, inhibition of bacterial entry occurred at the prevacuole stage: the bacteria were fully encircled by host membranes that retained $PI(4,5)P_2$ (Figures 2C, S2A, and S2D) but were unable to fuse and undergo scission (Figures 2F and 2F′). It is noteworthy that, in cells treated with PI3K inhibitors, many of the bacteria were inaccessible

to extracellular antibodies, confirming that arrest occurred at the prevacuolar stage. Specifically, 41.7% of bacteria in LY294002-treated cells were inaccessible to antibody compared to 20.3% of bacteria inaccessible to streptavidin under the same conditions.

We confirmed that class I PI3Ks are active at sites of invasion by using the PH domain of Akt fused to GFP (PH-Akt), a probe for $PI(3,4,5)P_3$ and/or $PI(3,4)P_2$. In cells infected with *Y. pseudotuberculosis*, the probe was consistently recruited to forming vacuoles (Figure 3A) and this recruitment was obliterated by LY294002 (Figure 3B). As described earlier (Wong and Isberg, 2003), $PI(3,4,5)P_3$ and/or $PI(3,4)P_2$ persisted in sealed vacuoles, whereas $PI(4,5)P_2$ was removed more rapidly (Figures 3D and 3C, respectively).

Taken together, the preceding results imply that $PI(4,5)P_2$ disappears at the time of prevacuolar sealing and that scission requires formation of PI3K products. Because LY294002 and wortmannin not only prevented the appearance of $PI(3,4,5)P_3$ and/or $PI(3,4)P_2$ but also the elimination of $PI(4,5)P_2$ from the vacuole, it was unclear whether PI3Ks are directly involved in the scission process or act indirectly by stimulating the disappearance of $PI(4,5)P_2$. We discerned between these possibilities using a heterodimerization system to recruit the phosphatase domain from the yeast Inp54 inositol 5-phosphatase to the plasma membrane (Suh et al., 2006) (Figure 3E). Because dimerization is induced by the addition of rapamycin, we were able to initiate $PI(4,5)P_2$ hydrolysis at a time of our choice (Figure S3A). Cells expressing the Inp54 inositol 5-phosphatase heterodimerization system were infected with *Yersinia* with or without prior addition of LY294002 to inhibit PI3K. As expected, invasion occurred in cells treated with vehicle (DMSO) only but was greatly inhibited by LY294002 and stalled at the prevacuolar stage (Figure 3F). Subsequent addition of rapamycin to induce $PI(4,5)P_2$ hydrolysis had little effect on the controls but markedly stimulated invasion in cells where PI3K was inhibited (Figure 3F). Similar results were observed with a different rapamycin heterodimerization system that employed a mammalian 5-phosphatase domain (Figure S3B). Jointly, these results indicate that PI3K products are dispensable for invasion and that disappearance of $PI(4,5)P_2$ is the critical step in scission of the prevacuole. They also imply that the role of PI3K must be indirect, likely catalyzing the elimination of $PI(4,5)P_2$.

PLC Does Not Contribute Significantly to the Depletion of PI(4,5)P$_2$

We analyzed the possible contribution of PLCγ, an active $PI(4,5)P_2$ lipase that is stimulated by the products of PI3K (Rameh et al., 1998). Inhibition of PLC activity using U73122 did not significantly increase the number of bacteria found in $PI(4,5)P_2$-containing prevacuoles (Figure 2C), nor did it markedly affect bacterial entry into host cells (Figure 2E). Production of DAG at sites of invasion –analyzed using the C1 domain of PKCδ tagged with GFP– was detected in less than 5% of the events studied (Figures S2F and S2G). In these experiments the sensitivity of the probe was validated by addition of phorbol esters, which invariably recruited the DAG biosensor to the membrane (Figure S2I), and by using IgG-opsonized sheep red blood cells (SRBC-IgG) as positive controls (Figures S2F and S2H). Fcγ receptor-mediated engulfment of SRBC-IgG is associated with generation of DAG (Botelho et al., 2000). Lastly, we did not observe appreciable recruitment of PLCγ1 or PLCγ2 to sites of bacterial entry, nor could we detect activation of PLCγ1, PLCγ2, or any of the PKC

isoforms in lysates of cells infected with *Yersinia* using phospho-specific antibodies (not illustrated). Jointly, these data argue against a major role for PLC-mediated hydrolysis of $PI(4,5)P_2$ in the bacterial entry process.

Recruitment of PI(4,5)P$_2$ Phosphatases to Sites of *Yersinia* Infection

Several $PI(4,5)P_2$ phosphatases, including oculocerebrorenal syndrome of Lowe protein (OCRL) and Inpp5b, have been implicated in endocytosis (Shin et al., 2005; Erdmann et al., 2007). To determine whether any of these phosphatases are involved in *Yersinia* entry, we investigated whether they are recruited to sites of infection, using GFP-tagged constructs. We observed recruitment of OCRL (Figure 4A) and Inpp5b (Figures S4A and S4A′) to nascent vacuoles. OCRL and Inpp5b were acquired quickly, reaching maximal accumulation 10–20 min after infection (Figures 4B and S4B). In some instances, FM4-64-positive vacuoles had already acquired OCRL (Figure 4A′), implying that the phosphatase was recruited prior to sealing, consistent with a role in the scission process.

To directly test whether OCRL and Inpp5b promote *Yersinia* entry through their ability to hydrolyze $PI(4,5)P_2$ (Matzaris et al., 1994; Zhang et al., 1995), we silenced their expression using siRNA (Figures 4C and 4D). *Yersinia* entry into the cells, defined by exclusion of streptavidin, was partially inhibited upon knockdown of either OCRL or Inpp5b (Figure 4E). Simultaneous knockdown of both phosphatases had an additive effect. Thus, depletion of $PI(4,5)P_2$ by these 5-phosphatases is associated with, and may be responsible for, the scission of vacuoles during *Yersinia* entry into host cells.

Rab5 Recruits OCRL and Inpp5b to the Invasion Vacuole and Is Required for Bacterial Entry

OCRL and Inpp5b are effectors of Rab5 (Hyvola et al., 2006), raising the possibility that this GTPase may be involved in bacterial invasion. There is no information linking Rab5 to *Yersinia* entry and little is known regarding the timing and mechanism of Rab5 association with the vacuole. Using a specific antibody, we detected endogenous Rab5 on *Yersinia*-containing vacuoles shortly after infection of COS cells (Figure 5A). We then used Rab5-GFP to monitor continuously the recruitment of the GTPase to sites of *Yersinia* invasion. As illustrated in Figures 5B and 5C, Rab5 recruitment recapitulates the kinetics described for OCRL and Inpp5b, which becomes apparent atforming vacuoles within 5 min and reaching maximal levels 10–20 min after exposure to bacteria. Indeed, when coexpressed in COS cells, Rab5-GFP and OCRL-mRuby colocalized essentially 100% of the time at sites of bacterial uptake (Figure 5D and data not shown).

The functional relationship between these proteins was studied using a dominant-negative form of Rab5 (Rab5[S34N]). Notably, in cells expressing Rab5(S34N) neither OCRL nor Inpp5b were recruited to sites where bacteria associated with the cells for up to 1 hr after infection (Figures 5E, 5F, S5A, and S5B). Thus, active Rab5 appears to be essential for OCRL and Inpp5b recruitment to vacuoles during *Yersinia* entry.

Based on the preceding results, we hypothesized that Rab5 recruits OCRL and Inpp5b to sites of invasion and that these phosphatases mediate, at least in part, the removal of

PI(4,5)P$_2$ required for scission of the prevacuole. This implies that Rab5, which is normally required for maturation of formed vacuolar/phagocytic compartments, also has a role at an earlier stage of the process (i.e., during bacterial entry). This notion was tested by measuring the effects of dominant-negative Rab5 on invasion. Strikingly, and consistent with our hypothesis, we found that expression of Rab5(S34N) inhibited *Yersinia* entry, assessed using the FM4-64 accessibility assay, whereas similar expression of the wild-type allele of Rab5 was without effect (Figure 6C). Virtually identical results were obtained when Rab5 was silenced using siRNA and entry was determined using streptavidin (Figure 6D). Note that, to circumvent possible functional redundancy, all three isoforms of Rab5 (A, B and C) were simultaneously silenced in these experiments.

Our hypothesis also predicts that, by precluding the recruitment of the phosphatases, inactivation of Rab5 must have resulted in persistence of PI(4,5)P$_2$ in the membrane, thereby impairing scission and causing arrest at the prevacuolar stage. These predictions were also tested experimentally in cells transfected with Rab5(S34N). As shown in Figures 6A and 6B, we noted a marked increase in the number of PI(4,5)P$_2$-positive pre-vacuoles in cells expressing the dominant-negative allele compared to wild-type Rab5. In cells transfected with Rab5(S34N), PI(4,5)P$_2$ persisted on the prevacuolar membrane for up to 30 min (Figure 6A).

The occurrence of arrest at the prevacuolar stage was validated by TEM in cells subjected to siRNA silencing of all three Rab5 isoforms. As illustrated in Figure 6E, binding of *Yersinia* and extension of pseudopods that encircled the bacteria still occurred in cells depleted of Rab5, ruling out wholesale deleterious effects. Instead, vacuole formation was prevented by the inability of the membranes to fuse and undergo scission, in all likelihood as a consequence of the persistence of PI(4,5)P$_2$. Taken together, these data suggest that Rab5 is required for the final step of *Yersinia* entry into host cells.

Rab5 is Recruited to *Yersinia* Prevacuoles Prior to scission from the Plasma Membrane

Next, we used live imaging to examine the dynamics of Rab5 during invasion. To compare the kinetics of acquisition of the GTPase with the course of disappearance of PI(4,5)P$_2$, we cotransfected COS cells with plasmids encoding Rab5-GFP and RFP-tagged PH-PLCδ. As reported above, PI(4,5)P$_2$ was observed lining the membrane at sites of *Yersinia* entry (Figures 7A and 7A′). Importantly, in the majority (>90%) of cases, Rab5-containing vesicles were observed to be recruited and seemingly fused with the prevacuolar membrane, where PI(4,5)P$_2$ was still present, possibly contributing to its removal. PI(4,5)P$_2$ was found to disappear from the prevacuoles within seconds of their association with Rab5 (Figures 7A, 7A′, S7A, and Movie S1A). Recruitment of Rab5 to the vacuole progressed thereafter, reaching a maximum level on average 36.9 ± 15.6 s after association was initially detectable. Furthermore, immunostaining revealed accumulation of endogenous Rab5 on prevacuoles with detectable PI(4,5)P$_2$ (Figure S7B). The PI(4,5)P$_2$ content of Rab5-positive prevacuoles was lower than that of vacuoles that had not yet accumulated Rab5 (compare open with closed arrowheads in Figure S7B), consistent with a role of the GTPase in promoting disappearance of PI(4,5)P$_2$. This disappearance was most likely mediated by OCRL and/or Inpp5b because the kinetics of recruitment of these phosphatases mirrored that of Rab5. As

shown in Figures S6A, S6B, Movie S1B, and Movie S1C, OCRL and Inpp5b were similarly detectable on vesicles that associated with $PI(4,5)P_2$-containing prevacuoles, which appeared to fuse as the phosphoinositide vanished. These data strongly suggest that Rab5 recruitment to prevacuoles delivers phosphatases that dephosphorylate $PI(4,5)P_2$, facilitating membrane scission and thereby allowing bacterial entry.

PI3Ks Are Required for Fusion of Rab5-Positive Vesicles with the Prevacuole

Because PI3K inhibitors blocked the scission of prevacuoles, we tested their effect on the recruitment and fusion of Rab5-containing vesicles. When cells were treated with LY294002, we observed recruitment of Rab5-positive vesicles to the surface of $PI(4,5)P_2$-positive vacuoles (Figure 7B). However, the docked vesicles were unable to fuse with the vacuolar membrane (Figures 7B, 7C, and Movie S1D) and, as reported above, $PI(4,5)P_2$ persisted on the vacuolar membrane for extended periods of time. These results suggest that fusion of Rab5-positive vesicles requires the products of PI3K and that this event is essential for the recruitment of OCRL and Inpp5b and the subsequent hydrolysis of $PI(4,5)P_2$ that mediates vacuolar fission.

Discussion

The salient finding of our studies is the existence of an intermediate stage in the invasion process of *Yersinia*, the prevacuole, wherein bacteria are fully encircled by host membranes and segregated from large extracellular macromolecules. Unlike the fully formed vacuole, however, the prevacuole has not undergone scission from the plasmalemma and is richly endowed with $PI(4,5)P_2$. Indeed, disappearance of $PI(4,5)P_2$ coincides with and is required for scission. Moreover, we report that Rab5 associates with the prevacuoles and mediates the recruitment of OCRL and Inpp5b, contributing to the elimination of $PI(4,5)P_2$ and, thereby, to vacuolar fission. Lastly, we found that PI3K activity is essential for the recruitment of Rab5 and of the phosphatases. These observations are discussed in turn below.

While $PI(4,5)P_2$ is constitutively present in the plasma membrane, the phosphoinositide has been shown to undergo localized accumulation at sites of particle internalization, including that of *Yersinia* by epithelial cells (Wong and Isberg, 2003). The focal increase in $PI(4,5)P_2$ likely acts to recruit actin-remodeling proteins, allowing the membrane to extend around the target particle. In the case of *Yersinia*, increased $PI(4,5)P_2$ has been attributed to localized activation of PIP5Ks by Rac and Arf6 (Wong and Isberg, 2003). The initial accumulation of $PI(4,5)P_2$ at sites of bacterial internalization is followed by acute disappearance of the phosphoinositide upon membrane sealing. Remarkably, this feature is common to a variety of internalization processes, including endocytosis (Di Paolo and De Camilli, 2006), macropinocytosis (Porat-Shliom et al., 2008), and phagocytosis (Botelho et al., 2000). However, the functional significance of $PI(4,5)P_2$ hydrolysis is not fully understood. In the case of endocytosis, loss of $PI(4,5)P_2$ is thought to be required for the uncoating of clathrin-coated vesicles (Cremona et al., 1999). For phagosomes and macropinosomes, which are devoid of clathrin coats, $PI(4,5)P_2$ degradation has been speculated to promote clearance of F-actin, allowing membrane invagination (Scott et al., 2005). However, these proposed functions differ from the role described herein for bacterial invasion, wherein hydrolysis of

PI(4,5)P$_2$ by phosphatases appears to be essential for fission. It is noteworthy that, in a recent publication, artificially imposed dephosphorylation of PI(4,5)P$_2$ sufficed to induce fragmentation of tubules generated by overexpression of endophilin, a BAR domain-containing protein (Chang-Ileto et al., 2011). Several mechanisms can be envisaged to favor membrane scission: 1) the detachment of PI(4,5)P$_2$-binding (cytoskeletal?) proteins required for membrane stability; 2) a change in the curvature of the membrane resulting from the reduced bulk of the phosphoinositide headgroup; and/or 3) alterations in the surface charge that may facilitate apposition of curved membranes.

While PI(4,5)P$_2$ depletion is a common feature of several endocytic processes, the mechanism whereby the phosphoinositide is removed may vary in each instance. PI(4,5)P$_2$ can be metabolized by cells via multiple pathways, including: 1) hydrolysis by PLC to produce inositol 3,4,5-trisphosphate and DAG; 2) conversion to the signaling lipid PI(3,4,5)P$_3$ by PI3K; and 3) removal of the 4′ or 5′ phosphate moieties through the action of inositol polyphosphate 4- or 5-phosphatases. During Fcγ receptor-mediated phagocytosis, PI(4,5)P$_2$ disappearance correlates with DAG production and engulfment is inhibited by U73122, a PLC antagonist (Botelho et al., 2000; Scott et al., 2005). However, phagocytosis mediated by scavenger receptors is insensitive to U73122 (Sulahian et al., 2008). In contrast, clathrin-mediated endocytosis involves phosphatase-mediated degradation of PI(4,5)P$_2$ (Cremona et al., 1999; Mani et al., 2007; Shin et al., 2005), which parallels our observations during *Yersinia* invasion. Of note, the phosphatases responsible for PI(4,5)P$_2$ degradation during invasion need not be intrinsic to the host cell. Like *Yersinia*, *Salmonella* also invades epithelial cells and the entry process is similarly accompanied by acute disappearance of PI(4,5)P$_2$ (Terebiznik et al., 2002). In this instance, the hydrolysis of PI(4,5)P$_2$ has been attributed to the *Salmonella* effector SopB, which displays inositol polyphosphate 4-phosphatase activity (Mallo et al., 2008).

Perhaps the most unanticipated finding was the observation that Rab5 was recruited to incompletely sealed PI(4,5)P$_2$-positive prevacuoles. This GTPase is a marker of early endocytic vesicles and is typically regarded to direct their traffic, controlling fusion events and cytoskeletal transport (Gorvel et al., 1991; Bucci et al., 1992). Nevertheless, Rab5-containing vesicles were found to be recruited to F-actin-associated, extracellular *Staphylococcus* (Schröder et al., 2006) and Porat-Shliom et al. (2008) showed evidence of Rab5 association with forming macropinosomes prior to the loss of PI(4,5)P$_2$, in a manner similar to what we observed in the present study. Moreover, Rab5 activity is required for optimal endocytosis (Bucci et al., 1992; Stenmark et al., 1994) and fluid-phase uptake (Li et al., 1997; Lanzetti et al., 2004; Schnatwinkel et al., 2004), although the underlying mechanism is far from clear. Inasmuch as these processes involve the conversion of PI(4,5)P$_2$, it is conceivable that recruitment of phosphatases and depletion of the phosphoinositide may be involved.

It is unclear how Rab5 is recruited to the forming *Yersinia* vacuoles. Though difficult to visualize, some Rab5 may be present constitutively at the plasma membrane, where it could be activated by GEFs, such as RME-6 (Sato et al., 2005; Semerdjieva et al., 2008). This possibility is illustrated schematically in Figure 7D (1a and 1b). Activated Rab5 would, in turn, recruit OCRL and Inpp5b (Figure 7D [2a]). Active Rab5 could also reach the vacuole

through vesicular fusion (Figure 7D [2b]). These possibilities are not mutually exclusive. In fact, the presence of small amounts of Rab5 on the prevacuolar membrane may be required to form a bridge with Rab5-positive endosomes via EEA1 or similar adaptors. OCRL and Inpp5b could be recruited to the membrane directly by Rab5 or via the adaptor APPL1 (Erdmann et al., 2007). Indeed, as illustrated in Figures S4C and S4C′, APPL1 is readily detectable in nascent *Yersinia* vacuoles, where it colocalizes with OCRL and Inpp5b. Irrespective of how the phosphatases are recruited, $PI(4,5)P_2$ would then be removed and scission of the prevacuole from the plasma membrane would ensue, forming a sealed structure (Figure 7D [3]).

We found that fusion of Rab5-containing vesicles with the pre-vacuole requires active PI3K. Inhibition of PI3K also interferes with phagocytosis, seemingly by precluding the delivery of endo-membranes (Araki et al., 1996; Cox et al., 1999). However, whether Rab5-containing vesicles are directed to sites of phagosome formation is not known. Moreover, PI3K inhibitors arrest phagocytosis at a comparatively early stage by preventing the full extension of pseudopods, rather than scission of a nearly complete vacuole. Thus, PI3K isoforms appear to play multiple roles in particle engulfment.

In summary, our experiments point to a role of Rab5 and the associated phosphatases OCRL and Inpp5b in membrane scission, which may apply not only to specific instances of bacterial invasion but more widely to internalization processes like macropinocytosis and certain forms of endocytosis.

Experimental Procedures

Cell Culture and Transfection

HeLa and COS cells (passage number 5–30) were maintained in RPMI-1640 with 5% FBS, and in DMEM with 5% FBS (Wisent), respectively. Cells were plated on 18 mm glass coverslips (for live-cell imaging) or 12 mm coverslips (for experiments in which cells were fixed), prior to transfection. Cells at approximately 50% confluence were transfected with FuGENE 6 (Roche) and used between 18 and 24 hr posttransfection.

Preparation of Bacteria

The *Yersinia pseudotuberculosis* strain used in this study was the virulence plasmid-cured (P⁻) YPIII. Bacteria were cultured as described by Wong and Isberg (2003). For live-cell imaging, bacteria were labeled with 20 μg of Alexa 647 succinimidyl ester (Invitrogen) in 500 μl of 100 mM sodium bicarbonate buffer, pH 8.5, for 10 min at room temperature. Biotinylation of bacteria was performed with EZ-Link NHS-LC-Biotin (0.2 mg) (Pierce) in 500 μl phosphate-buffered saline (PBS), pH 8, for 30 min at room temperature, followed by quenching in 500 μl of PBS+100 mM glycine for 10 min at room temperature. Biotinylated bacteria were then labeled with Alexa 647 as above.

Infection of Cells

Prior to infection, cells were washed twice with serum-free medium. Where indicated, cells were pretreated with inhibitors as follows: 3 μM U73122 (Sigma), 50 μM LY294002 (Enzo

Life Sciences), 100 nM wortmannin (Calbiochem), or an equal volume of the solvent, DMSO (Sigma); inhibitors were maintained in the medium throughout infections. For rapamycin heterodimerization, 1 μM rapamycin (Sigma) was added to cells infected in the presence of LY294002 for 30 min. Prior to infection in experiments with C1-PKCδ or PH-Akt, cells were serum-starved at least 3 hr. In all cases, cells were infected with bacteria at a multiplicity of infection of 150:1. Bacteria were centrifuged onto cells for 1 min at $277 \times g$ to facilitate binding, and cells were washed twice to remove unbound bacteria. Following these manipulations, 25–50 bacteria, on average, remained associated with the cells. Infections were then allowed to proceed at 37°C for indicated durations.

Streptavidin and FM4-64 Labeling

Where indicated, samples were fixed after infection with 3.7% paraformaldehyde (PFA; Electron Microscopy Sciences) in PBS, for 15 min at room temperature. For streptavidin staining, infections were stopped on ice and fluorescent streptavidin conjugates (Invitrogen) were added at 5 μg/ml in PBS with 0.4% BSA for 10 min on ice. Cells were then washed twice with PBS, fixed with PFA, and mounted for imaging using Fluorescent Mounting Medium (Dako). Antibody staining of extracellular *Yersinia* was conducted with rabbit anti-*Yersinia* antibody (Agrisera) at 1/1,000 in blocking solution, followed by a fluorescent secondary antibody (Jackson ImmunoResearch). For live-cell imaging, cells were washed twice in HEPES-buffered RPMI 1640 (HPMI; Wisent) and imaged in the same medium. For FM4-64 staining, cells were washed on ice with cold HPMI, and FM4-64 (Invitrogen) was added to a final concentration of 5 μg/ml. Cells were imaged quickly (<5 min) in ice-cold HPMI to minimize internalization of the dye.

Data Presentation and Statistical Analyses

Graphs show the mean ± SEM of at least three independent experiments conducted on separate days; at least 15 cells with 20 bacteria per cell, on average, were counted for each condition in every experiment. Statistical analyses were performed using two-tailed equal variance Student's t tests for samples where two sets of means were compared, or using 1-way ANOVA followed by Dunnett's post test where more than two sets of means were compared; p values are indicated as * < 0.05, ** < 0.001.

Supplementary Material

Refer to Web version on PubMed Central for supplementary material.

Acknowledgments

References

Alrutz MA, Srivastava A, Wong KW, D'Souza-Schorey C, Tang M, Ch'Ng LE, Snapper SB, Isberg RR. Efficient uptake of Yersinia pseudotuberculosis via integrin receptors involves a Rac1-Arp 2/3 pathway that bypasses N-WASP function. Mol Microbiol. 2001; 42:689–703. [PubMed: 11722735]

Araki N, Johnson MT, Swanson JA. A role for phosphoinositide 3-kinase in the completion of macropinocytosis and phagocytosis by macrophages. J Cell Biol. 1996; 135:1249–1260. [PubMed: 8947549]

Botelho RJ, Teruel M, Dierckman R, Anderson R, Wells A, York JD, Meyer T, Grinstein S. Localized biphasic changes in phosphatidylinositol-4,5-bisphosphate at sites of phagocytosis. J Cell Biol. 2000; 151:1353–1368. [PubMed: 11134066]

Bucci C, Parton RG, Mather IH, Stunnenberg H, Simons K, Hoflack B, Zerial M. The small GTPase rab5 functions as a regulatory factor in the early endocytic pathway. Cell. 1992; 70:715–728. [PubMed: 1516130]

Chang-Ileto B, Frere SG, Chan RB, Voronov SV, Roux A, Di Paolo G. Synaptojanin 1-mediated PI(4,5)P2 hydrolysis is modulated by membrane curvature and facilitates membrane fission. Dev Cell. 2011; 20:206–218. [PubMed: 21316588]

Cox D, Tseng CC, Bjekic G, Greenberg S. A requirement for phosphatidylinositol 3-kinase in pseudopod extension. J Biol Chem. 1999; 274:1240–1247. [PubMed: 9880492]

Cremona O, Di Paolo G, Wenk MR, Lüthi A, Kim WT, Takei K, Daniell L, Nemoto Y, Shears SB, Flavell RA, et al. Essential role of phosphoinositide metabolism in synaptic vesicle recycling. Cell. 1999; 99:179–188. [PubMed: 10535736]

Di Paolo G, De Camilli P. Phosphoinositides in cell regulation and membrane dynamics. Nature. 2006; 443:651–657. [PubMed: 17035995]

Erdmann KS, Mao Y, McCrea HJ, Zoncu R, Lee S, Paradise S, Modregger J, Biemesderfer D, Toomre D, De Camilli P. A role of the Lowe syndrome protein OCRL in early steps of the endocytic pathway. Dev Cell. 2007; 13:377–390. [PubMed: 17765681]

Gorvel JP, Chavrier P, Zerial M, Gruenberg J. rab5 controls early endosome fusion in vitro. Cell. 1991; 64:915–925. [PubMed: 1900457]

Herre J, Marshall AS, Caron E, Edwards AD, Williams DL, Schweighoffer E, Tybulewicz V, Reis e Sousa C, Gordon S, Brown GD. Dectin-1 uses novel mechanisms for yeast phagocytosis in macrophages. Blood. 2004; 104:4038–4045. [PubMed: 15304394]

Huynh KK, Kay JG, Stow JL, Grinstein S. Fusion, fission, and secretion during phagocytosis. Physiology (Bethesda). 2007; 22:366–372. [PubMed: 18073409]

Hyvola N, Diao A, McKenzie E, Skippen A, Cockcroft S, Lowe M. Membrane targeting and activation of the Lowe syndrome protein OCRL1 by rab GTPases. EMBO J. 2006; 25:3750–3761. [PubMed: 16902405]

Isberg RR, Leong JM. Multiple beta 1 chain integrins are receptors for invasin, a protein that promotes bacterial penetration into mammalian cells. Cell. 1990; 60:861–871. [PubMed: 2311122]

Lanzetti L, Palamidessi A, Areces L, Scita G, Di Fiore PP. Rab5 is a signalling GTPase involved in actin remodelling by receptor tyrosine kinases. Nature. 2004; 429:309–314. [PubMed: 15152255]

Li G, D'Souza-Schorey C, Barbieri MA, Cooper JA, Stahl PD. Uncoupling of membrane ruffling and pinocytosis during Ras signal transduction. J Biol Chem. 1997; 272:10337–10340. [PubMed: 9099668]

Mallo GV, Espina M, Smith AC, Terebiznik MR, Alemán A, Finlay BB, Rameh LE, Grinstein S, Brumell JH. SopB promotes phosphatidylinositol 3-phosphate formation on Salmonella vacuoles by recruiting Rab5 and Vps34. J Cell Biol. 2008; 182:741–752. [PubMed: 18725540]

Mani M, Lee SY, Lucast L, Cremona O, Di Paolo G, De Camilli P, Ryan TA. The dual phosphatase activity of synaptojanin1 is required for both efficient synaptic vesicle endocytosis and reavailability at nerve terminals. Neuron. 2007; 56:1004–1018. [PubMed: 18093523]

Matzaris M, Jackson SP, Laxminarayan KM, Speed CJ, Mitchell CA. Identification and characterization of the phosphatidylinositol-(4, 5)-bisphosphate 5-phosphatase in human platelets. J Biol Chem. 1994; 269:3397–3402. [PubMed: 8106379]

Porat-Shliom N, Kloog Y, Donaldson JG. A unique platform for H-Ras signaling involving clathrin-independent endocytosis. Mol Biol Cell. 2008; 19:765–775. [PubMed: 18094044]

Rameh LE, Rhee SG, Spokes K, Kazlauskas A, Cantley LC, Cantley LG. Phosphoinositide 3-kinase regulates phospholipase Cgamma-mediated calcium signaling. J Biol Chem. 1998; 273:23750–23757. [PubMed: 9726983]

Rosenshine I, Duronio V, Finlay BB. Tyrosine protein kinase inhibitors block invasin-promoted bacterial uptake by epithelial cells. Infect Immun. 1992; 60:2211–2217. [PubMed: 1587588]

Sato M, Sato K, Fonarev P, Huang CJ, Liou W, Grant BD. Caenorhabditis elegans RME-6 is a novel regulator of RAB-5 at the clathrin-coated pit. Nat Cell Biol. 2005; 7:559–569. [PubMed: 15895077]

Schnatwinkel C, Christoforidis S, Lindsay MR, Uttenweiler-Joseph S, Wilm M, Parton RG, Zerial M. The Rab5 effector Rabankyrin-5 regulates and coordinates different endocytic mechanisms. PLoS Biol. 2004; 2:E261. [PubMed: 15328530]

Schröder A, Schröder B, Roppenser B, Linder S, Sinha B, Fässler R, Aepfelbacher M. Staphylococcus aureus fibronectin binding protein-A induces motile attachment sites and complex actin remodeling in living endothelial cells. Mol Biol Cell. 2006; 17:5198–5210. [PubMed: 17021255]

Schulte R, Zumbihl R, Kampik D, Fauconnier A, Autenrieth IB. Wortmannin blocks Yersinia invasin-triggered internalization, but not interleukin-8 production by epithelial cells. Med Microbiol Immunol (Berl). 1998; 187:53–60. [PubMed: 9749983]

Scott CC, Dobson W, Botelho RJ, Coady-Osberg N, Chavrier P, Knecht DA, Heath C, Stahl P, Grinstein S. Phosphatidylinositol-4,5-bisphosphate hydrolysis directs actin remodeling during phagocytosis. J Cell Biol. 2005; 169:139–149. [PubMed: 15809313]

Semerdjieva S, Shortt B, Maxwell E, Singh S, Fonarev P, Hansen J, Schiavo G, Grant BD, Smythe E. Coordinated regulation of AP2 uncoating from clathrin-coated vesicles by rab5 and hRME-6. J Cell Biol. 2008; 183:499–511. [PubMed: 18981233]

Shin HW, Hayashi M, Christoforidis S, Lacas-Gervais S, Hoepfner S, Wenk MR, Modregger J, Uttenweiler-Joseph S, Wilm M, Nystuen A, et al. An enzymatic cascade of Rab5 effectors regulates phosphoinositide turnover in the endocytic pathway. J Cell Biol. 2005; 170:607–618. [PubMed: 16103228]

Stenmark H, Parton RG, Steele-Mortimer O, Lütcke A, Gruenberg J, Zerial M. Inhibition of rab5 GTPase activity stimulates membrane fusion in endocytosis. EMBO J. 1994; 13:1287–1296. [PubMed: 8137813]

Suh BC, Inoue T, Meyer T, Hille B. Rapid chemically induced changes of PtdIns(4,5)P2 gate KCNQ ion channels. Science. 2006; 314:1454–1457. [PubMed: 16990515]

Sulahian TH, Imrich A, Deloid G, Winkler AR, Kobzik L. Signaling pathways required for macrophage scavenger receptor-mediated phagocytosis: analysis by scanning cytometry. Respir Res. 2008; 9:59. [PubMed: 18687123]

Terebiznik MR, Vieira OV, Marcus SL, Slade A, Yip CM, Trimble WS, Meyer T, Finlay BB, Grinstein S. Elimination of host cell PtdIns(4,5)P(2) by bacterial SigD promotes membrane fission during invasion by Salmonella. Nat Cell Biol. 2002; 4:766–773. [PubMed: 12360287]

Vieira OV, Bucci C, Harrison RE, Trimble WS, Lanzetti L, Gruenberg J, Schreiber AD, Stahl PD, Grinstein S. Modulation of Rab5 and Rab7 recruitment to phagosomes by phosphatidylinositol 3-kinase. Mol Cell Biol. 2003; 23:2501–2514. [PubMed: 12640132]

Wong KW, Isberg RR. Arf6 and phosphoinositol-4-phosphate-5-kinase activities permit bypass of the Rac1 requirement for beta1 integrin-mediated bacterial uptake. J Exp Med. 2003; 198:603–614. [PubMed: 12925676]

Yeung T, Grinstein S. Lipid signaling and the modulation of surface charge during phagocytosis. Immunol Rev. 2007; 219:17–36. [PubMed: 17850479]

Young VB, Falkow S, Schoolnik GK. The invasin protein of Yersinia enterocolitica: internalization of invasin-bearing bacteria by eukaryotic cells is associated with reorganization of the cytoskeleton. J Cell Biol. 1992; 116:197–207. [PubMed: 1730744]

Zhang X, Jefferson AB, Auethavekiat V, Majerus PW. The protein deficient in Lowe syndrome is a phosphatidylinositol-4,5-bisphosphate 5-phosphatase. Proc Natl Acad Sci USA. 1995; 92:4853–4856. [PubMed: 7761412]
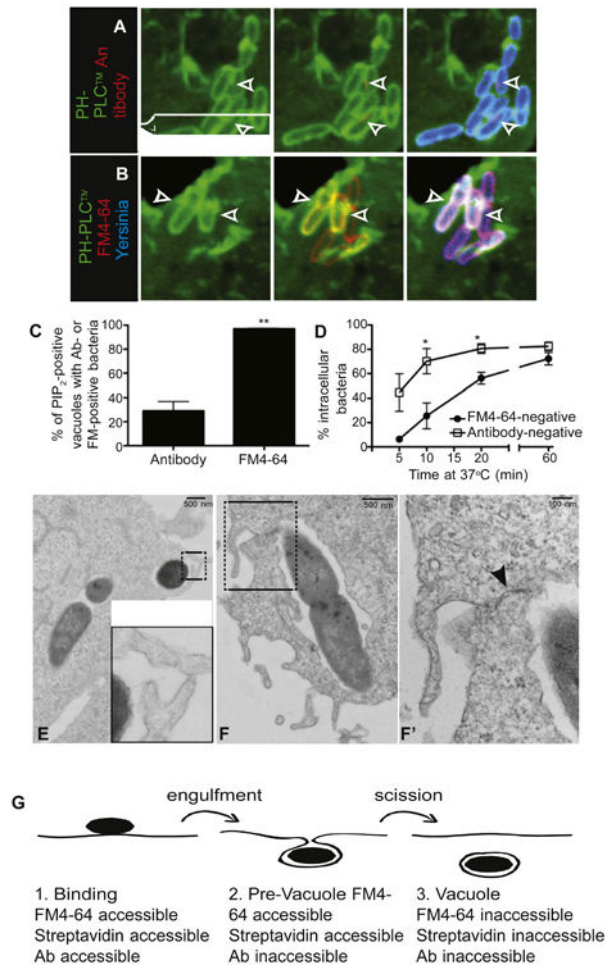
Figure 1. Identification of an Intermediate stage of *Yersinia* Entry into Host Cells

(A) Prior to vacuolar scission, *Yersinia* reside in PI(4,5)P$_2$-positive structures that are inaccessible to antibodies. COS cells expressing the PH domain of PLCδ fused to GFP (PH-PLCδ) were infected with Alexa 647-labeled *Y. pseudotuberculosis* (blue) for 10 min, followed by fixation and staining using antibody to *Yersinia*, followed by Alexa 546-conjugated secondary antibody (red). Arrowheads denote PI(4,5)P$_2$-positive vacuoles containing antibody-negative bacteria.

(B) PI(4,5)P$_2$-positive, *Yersinia*-containing structures are accessible to the extracellular marker FM4-64. COS cells expressing PH-PLCδ were infected with Alexa 647-labeled *Y. pseudotuberculosis* (blue) for 10 min, then cooled and stained with FM4-64 (red). Arrowheads denote PI(4,5)P$_2$-positive vacuoles containing FM4-64-positive (i.e., extracellularly accessible) bacteria.

(C) Bacteria in PI(4,5)P$_2$-positive structures are always accessible to FM4-64, whereas a minority is accessible to antibody. COS cells expressing PH-PLCδ were infected with *Yersinia* for 10 min, then stained with FM4-64 and imaged, followed by fixation and staining with antibody to *Yersinia*. In (C) and (D), data are means of three independent experiments. Error bars represent ± SEM.

(D) Quantification of invasion based on antibody accessibility overestimates entry. COS cells were infected with *Yersinia* for various times, followed by staining with FM4-64 and imaging. Cells were then fixed, stained with antibody, and images were quantified for entry.

(E and F) Identification of a late stage of *Yersinia* entry. COS cells were infected with *Yersinia* for 5 min, followed by fixation and processing of samples for TEM. Insets (E and F ′) represent magnified images of the areas denoted by boxes in (E) and (F), respectively. Arrowhead in F′ points to juxtaposed membranes that have not yet fused.

(G) Stages of *Yersinia* entry into cells. Binding of bacteria to cells without significant membrane envelopment constitutes the first, FM4-64-, streptavidin-, and antibody-accessible stage. This is followed by wrapping of membrane around bacteria, without fusion of the membranes; this is FM4-64- and streptavidin-accessible and antibody-inaccessible. Once scission occurs, the vacuole is internalized and therefore inaccessible to FM4-64, streptavidin, and antibody. See also Figure S1.
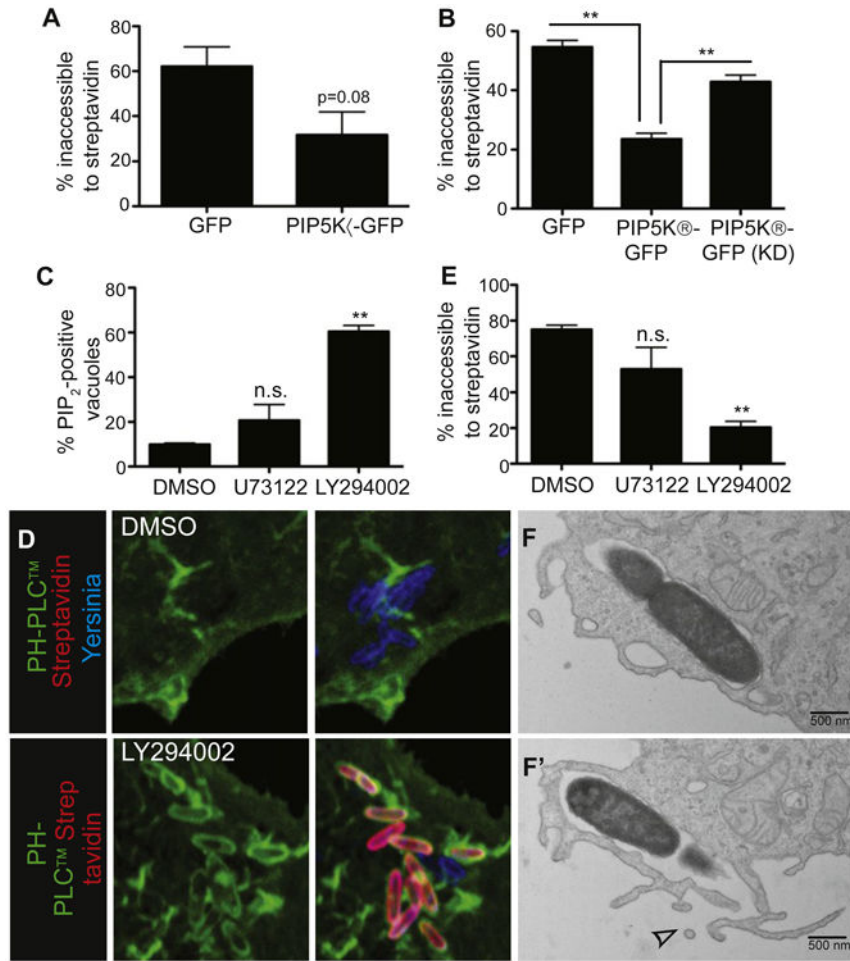
Figure 2. Loss of PI(4,5)P$_2$ and Scission of the *Yersinia*-Containing Vacuole from the Plasma Membrane Are PI3K-Dependent

(A) Overexpression of PIP5Kα inhibits *Yersinia* entry into cells. COS cells transfected with the indicated constructs were infected with biotinylated Alexa 647-labeled *Yersinia* for 30 min, then stained with Alexa 546-streptavidin before fixation and quantification of bacterial entry.

(B) Overexpression of PIP5Kβ, but not a kinase-dead (KD) mutant, inhibits *Yersinia* entry into cells. Experiment conducted as in (A).

(C and D) Inhibition of PI3K increases the proportion of *Yersinia* at the PI(4,5)P$_2$-containing stage. COS cells transfected with PH-PLCδ-GFP were treated with U73122, LY294002, or vehicle (DMSO), followed by infection with Alexa 647-labeled *Yersinia* for 30 min and fixation. PI(4,5) P$_2$-positive bacteria were then quantified. (D) shows representative images from (C).

(E) PI3K inhibition reduces *Yersinia* entry into host cells. COS cells were treated with inhibitors, then infected with biotinylated Alexa 647-labeled *Yersinia* for 30 min, followed by staining with Alexa 546-streptavidin and fixation. Images were quantified to assess bacterial entry. Data are means of three (A and B) or four (C and E) independent experiments. Error bars represent ± SEM.

(F) Inhibition of PI3K blocks *Yersinia* entry just prior to scission. LY294002-treated COS cells were infected with *Yersinia* for 10 min, followed by fixation and processing for TEM. (F) and (F′) are serial sections; top section shows a seemingly sealed vacuole, which revealed an opening to the extracellular space in the subsequent section (F′, see arrowhead). See also Figure S2.
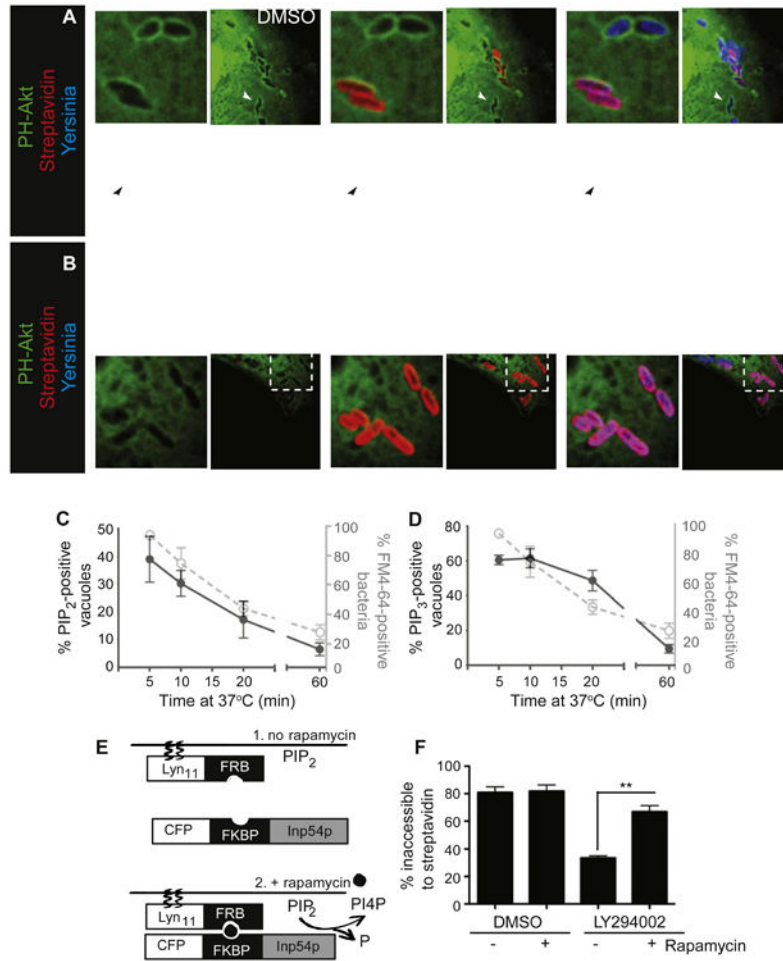
Figure 3. Elimination of PI(4,5)P$_2$, without Production of PI(3,4,5)P$_3$, Promotes *Yersinia* Entry

(A) PI(3,4,5)P$_3$ production during *Yersinia* infection. COS cells transfected with the PI(3,4,5)P$_3$-binding PH domain of Akt fused to GFP (PH-Akt) were infected with biotinylated Alexa 647-labeled *Yersinia* for 10 min, followed by staining with Alexa 546-streptavidin, fixation, and imaging. Solid arrowheads denote intracellular bacteria; open arrowheads denote extracellular bacteria.

(B) LY294002 inhibits production of PI(3,4,5)P$_3$ during *Yersinia* infection. Cells were treated with LY294002, followed by infection, staining, and imaging.

(C) Accessibility to FM4-64 diminishes in parallel with the disappearance of PI(4,5)P$_2$. COS cells transfected with PH-PLCδ were infected with *Yersinia*, and the fraction of vacuoles containing PI(4,5)P$_2$ determined over time. The fraction of vacuoles accessible to FM4-64, taken from experiments in Figure 1D, is shown in gray here and in D.

(D) PI(3,4,5)P$_3$ production does not parallel *Yersinia* entry. COS cells transfected with PH-Akt were infected and the fraction of vacuoles containing PI(3,4,5)P$_3$ determined as a function of time. Data in C, D, and F are means of three independent experiments. Error bars represent ± SEM.

(E) Schematic depiction of the rapamycin-based heterodimerization system used in (F). LDR consists of the plasma membrane-targeting sequence from Lynkinase (Lyn11) fused to

the N terminus of the FRB domain of mTOR1. Inp54-CFP consists of the 5-phosphatase domain of Inp54 (Inp54p) fused to CFP, as well as N-terminus of FKBP12 (FKBP). The components of the system are shown before (1) and after (2) rapamycin-induced dimerization.

(F) Recruitment of a PI(4,5)P$_2$-specific phosphatase to the plasma membrane promotes entry of bacteria trapped in PI(4,5)P$_2$-containing prevacuoles during PI3K inhibition. COS cells transfected with LDR and Inp54-CFP were treated with LY294002 or DMSO, then infected with biotinylated *Yersinia* for 30 min, at which point rapamycin was added to recruit the 5-phosphatase to the plasma membrane. Cells were incubated for another 10 min, followed by staining with streptavidin, fixation, and quantification of entry. See also Figure S3.
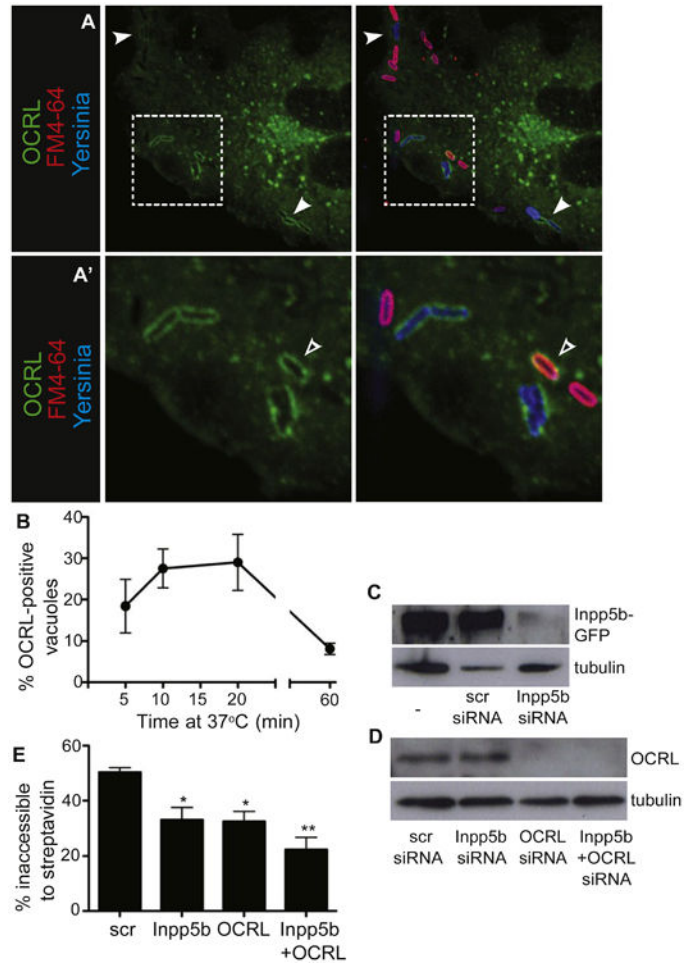
Figure 4. PI(4,5)P$_2$ Phosphatases Are Recruited to and Required for *Yersinia* Infection of Host Cells

(A and A′) OCRL is recruited to *Yersinia*-containing vacuoles during infection. COS cells were transfected with OCRL-GFP and infected with Alexa 647-labeled *Yersinia* for 10 min, followed by staining with FM4-64 and imaging.

(A) Arrowheads indicate *Yersinia*-containing vacuoles decorated with OCRL. (A′) is a magnified image of the area denoted by the box in (A); the open arrowhead denotes a vacuole that contains OCRL but is still accessible to FM4-64.

(B) Kinetics of OCRL recruitment to *Yersinia*. COS cells were transfected with OCRL-GFP and infected for various times with *Yersinia*, followed by fixation and quantification of OCRL-positive vacuoles. Data in B and E are means of three independent experiments. Error bars represent ± SEM.

(C and D) Confirmation of Inpp5b and OCRL knockdown in HeLa cells. (C) HeLa cells were transfected with Inpp5b-GFP, then left untreated (left lane) or treated with either scrambled (middle lane) or Inpp5b-targeted siRNA (right lane). Lysates were probed with antibody to GFP to detect Inpp5b-GFP. Tubulin was used as loading control. (D) HeLa cells were treated with siRNA as shown, and lysates probed with antibodies to detect endogenous OCRL (top) or tubulin (bottom) as a loading control.

(E) Inpp5b and OCRL knockdown inhibits *Yersinia* entry. HeLa cells were treated with siRNAs and infected 48 hr later with *Yersinia* for 30 min, followed by staining of extracellular bacteria with streptavidin, fixation, and quantification of entry. See also Figure S4.
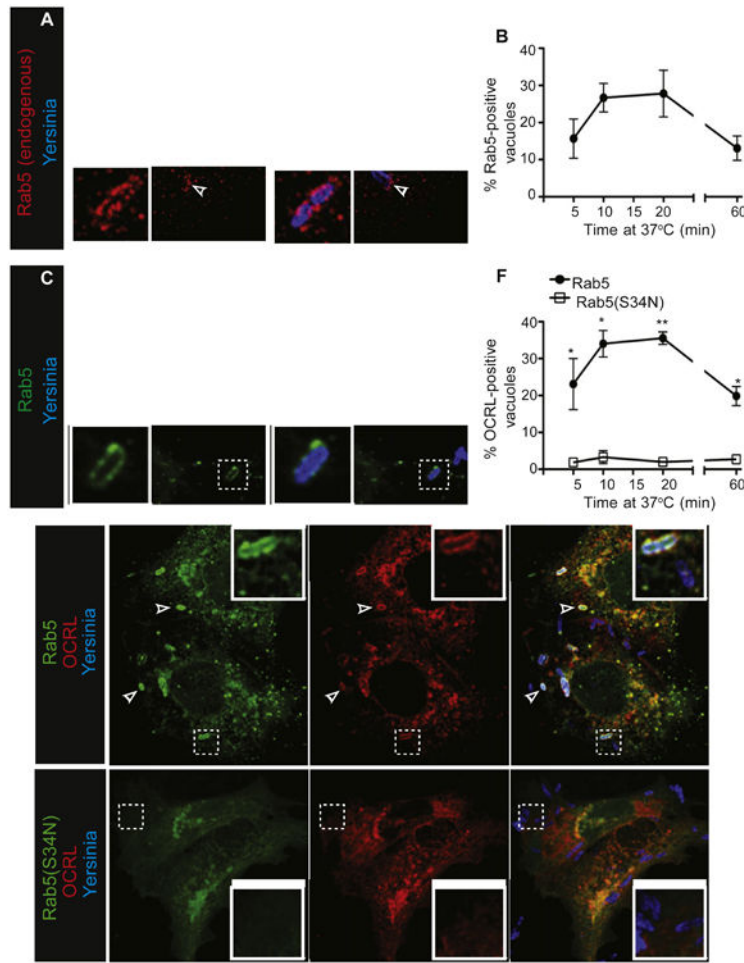
Figure 5. Rab5 Mediates the Recruitment of 5-Phosphatases to *Yersinia*-Containing Vacuoles
(A) Endogenous Rab5 is recruited to *Yersinia*-containing vacuoles. COS cells were infected with Alexa 647-labeled *Yersinia* for 10 min, followed by fixation, permeabilization, and staining with antibody to Rab5, followed by DyLight 549-conjugated secondary.
(B and C) Kinetics of Rab5 recruitment to *Yersinia*-containing vacuoles. (B) COS cells transfected with Rab5-GFP were infected with *Yersinia* for indicated times, followed by fixation and quantification of Rab5-positive vacuoles. Data in B and F are means of three independent experiments. Error bars represent ± SEM. (C) Image from (B), at 10 min.
(D–F) Active Rab5 is required for OCRL recruitment to *Yersinia* during infection. COS cells were transfected with wild-type Rab5-GFP and OCRL-mRuby (D) or Rab5(S34N)-GFP and OCRL-mRuby (E), then infected with Alexa 647-labeled *Yersinia* for 10 min, followed by fixation. (F) Quantitation of OCRL-positive *Yersinia*-containing vacuoles in the presence of Rab5 or Rab5(S34N). See also Figure S5.
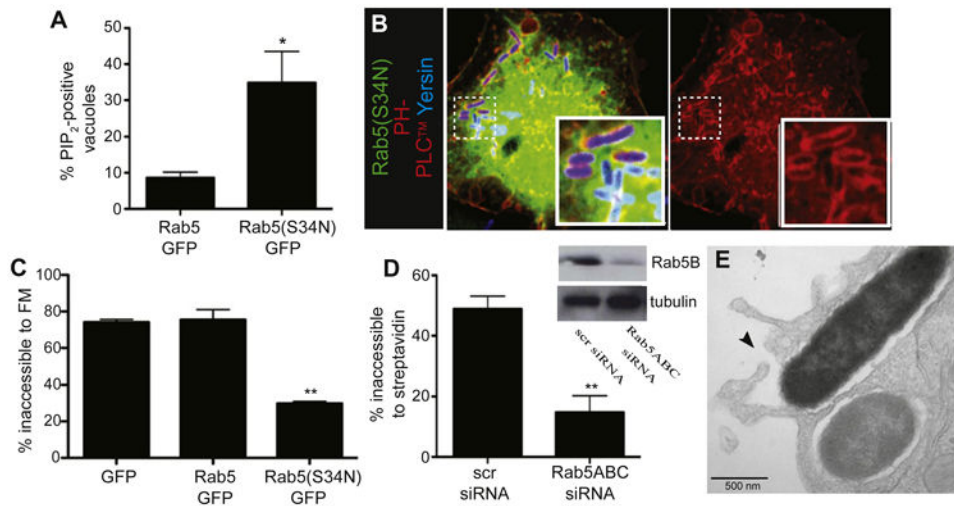
Figure 6. Rab5 Is Required for *Yersinia* Entry into Host Cells

(A) Dominant-negative Rab5 increases the proportion of PI(4,5)P$_2$-positive bacteria. COS cells were cotransfected with PH-PLCδ-RFP and either Rab5-GFP or Rab5(S34N)-GFP, and infected with Alexa 647-labeled *Yersinia* for 30 min, followed by fixation. Quantitation of PI(4,5)P$_2$-positive vacuoles. Data in (A), (C), and (D) are means of three independent experiments. Error bars represent ± SEM.

(B) Representative images from cells transfected with dominant-negative Rab5.

(C) Rab5(S34N) inhibits *Yersinia* entry into host cells. COS cells were transfected as shown, and infected with *Yersinia* for 30 min, followed by FM4-64 staining, imaging, and enumeration of intracellular bacteria.

(D) Rab5 is required for *Yersinia* entry. HeLa cells were treated with either scrambled or Rab5A,B,C-targeted siRNA, and infected 48 hr later with *Yersinia*. After infection, cells were stained with streptavidin and fixed, followed by enumeration of intracellular bacteria. Inset shows confirmation of Rab5B knockdown and tubulin control.

(E) Rab5 knockdown inhibits *Yersinia* entry at a late stage. HeLa cells were treated with siRNA to Rab5A,B,C and infected 48 hr later with *Yersinia* for 30 min, followed by fixation and processing for TEM. Arrowhead denotes juxtaposed, unfused membranes. See also Figure S7.
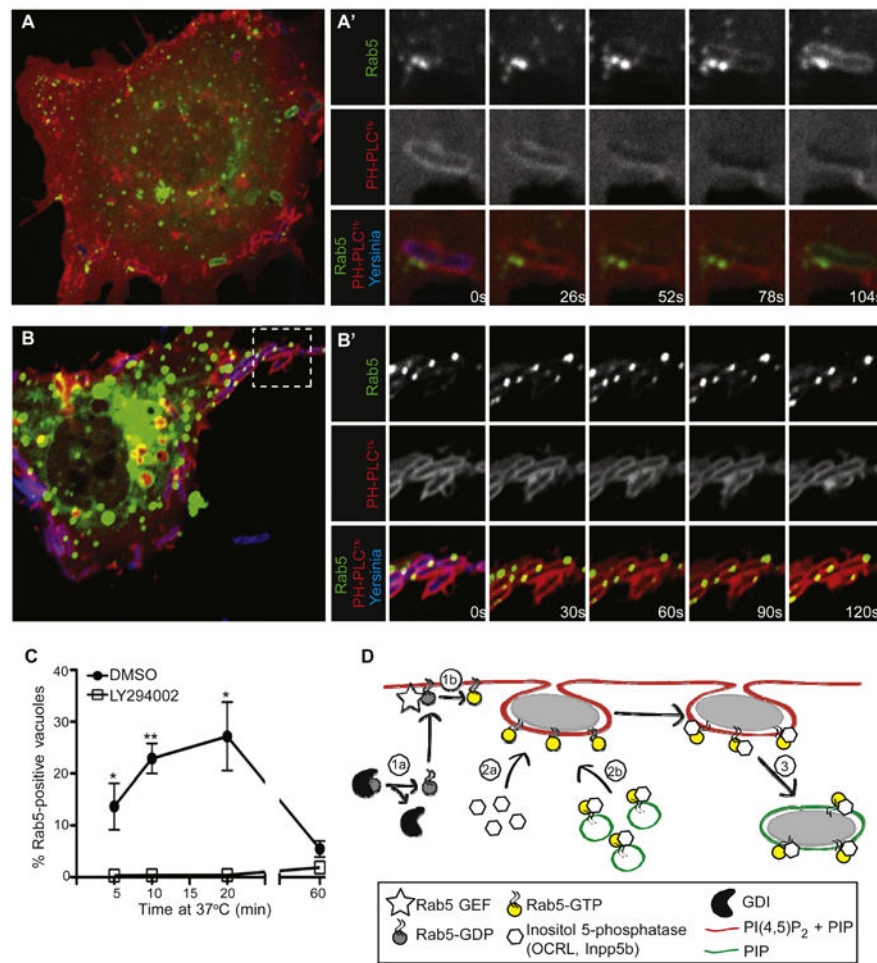
Figure 7. The Final Stages of *Yersinia* Entry into Host Cells Involve PI3K-Dependent Fusion of Rab5-Positive Vesicles with Prevacuoles

(A and A′) Rab5-positive vesicles are recruited to *Yersinia*-containing vacuoles seconds before PI(4,5)P$_2$ is lost from their membranes. COS cells were cotransfected with Rab5-GFP and PH-PLCδ-RFP, and infected with Alexa 647-labeled *Yersinia*. Images in A′ were acquired at 26 s intervals.

(B and B′) Rab5-positive vesicles are recruited but cannot fuse with PI(4,5)P$_2$-positive *Yersinia*-containing vacuoles in cells treated with LY294002. Experiment was conducted as in A, with images acquired every 30 s.

(C) COS cells were transfected with Rab5-GFP and treated with LY294002 or vehicle (DMSO) prior to infection for various times with *Yersinia*. Postinfection, cells were fixed, and Rab5-positive bacteria-containing vacuoles were quantified. Data are means of three independent experiments. Error bars represent ± SEM.

(D) Model of prevacuole scission. Rab5 may associate with the plasma membrane (1a), where it can be activated by plasma membrane-localized GEFs (1b), thereby allowing direct recruitment of OCRL or Inpp5b from the cytosol (2a). Alternatively (or additionally) endosomes bearing Rab5/OCRL/Inpp5b may fuse with the prevacuole membrane (2b).

Recruitment of OCRL/Inpp5b to prevacuoles results in hydrolysis of PI(4,5)P$_2$ and scission (3), generating a sealed vacuole. See also Figure S6 and Movie S1.